coatings

MDPI

Article

Structural and Optical Properties of CuO Thin Films Synthesized Using Spray Pyrolysis Method

Oleksii Diachenko [1,2,*], Jaroslav Kováč, Jr. [2], Oleksandr Dobrozhan [1], Patrik Novák [2], Jaroslav Kováč [2], Jaroslava Skriniarova [2] and Anatoliy Opanasyuk [1]

[1] Faculty of Electronics and Information Technologies, Sumy State University, 2, Rymsky Korsakov Str., 40007 Sumy, Ukraine; dobrozhan.a@gmail.com (O.D.); opanasyuk_sumdu@ukr.net (A.O.)
[2] Faculty of Electrical Engineering and Information Technology, Slovak University of Technology in Bratislava, Ilkovicova 3, 81219 Bratislava, Slovakia; jaroslav_kovac@stuba.sk (J.K.J.); patrik.novak@stuba.sk (P.N.); jaroslav.kovac@stuba.sk (J.K.); jaroslava.skriniarova@stuba.sk (J.S.)
* Correspondence: oleksii.di@gmail.com

Abstract: Copper oxide thin films were obtained using pulsating spray pyrolysis method. The morphological, structural, and optical properties of fabricated films were studied. X-ray analysis revealed that the CuO thin films are single-phase. The study of films morphology by SEM and AFM methods showed that the obtained films have a fairly high surface roughness and contain grains of different shapes and sizes. It was found that the obtained films of copper oxide have high values of the absorption coefficient, which confirms the possibility of their use as absorbing layers for solar cells. The obtained values of the optical band gap of the material are in the range from 1.45 eV to 1.60 eV. Raman spectroscopy revealed three modes A_{1g}, B_{1g}, and B_{2g}, of the crystal structure of monoclinic CuO. The devices based on *p*-type copper oxide are promising for solar cells fabrication because they can reduce production costs, due to their low cost and inexpensive production methods compared to silicon solar cells fabrication.

Keywords: copper oxide; films; X-ray; SEM; AFM analysis; optical properties; Raman spectroscopy

Citation: Diachenko, O., Kováč, J., Jr.; Dobrozhan, O.; Novák, P.; Kováč, J.; Skriniarova, J.; Opanasyuk, A. Structural and Optical Properties of CuO Thin Films Synthesized Using Spray Pyrolysis Method. *Coatings* **2021**, *11*, 1392. https://doi.org/10.3390/coatings11111392

Academic Editor: Alexandru Enesca

Received: 25 October 2021
Accepted: 13 November 2021
Published: 15 November 2021

1. Introduction

The rapid development of electronics requires using a variety of materials with the necessary physical, electrical, and optical characteristics to create modern devices. That is why scientists are paying more and more attention to studying new and already known chemical compounds that can exhibit semiconductor properties. Among such compounds, metal oxides can be considered the most promising [1]. These materials have several advantages over most other compounds when creating detectors, sensors, photovoltaic devices, and more. These advantages include environmental safety, non-toxicity, and chemical stability, allowing for obtaining materials directly in the environment. The composition of oxides, as a rule, contains elements that are widespread in the earth's crust, the methods of obtaining them are simple and require only low-temperature processing of the material. In addition, the oxide compounds themselves have a potentially lower cost due to inexpensive components and efficient and inexpensive production methods [2–4].

In recent years, a compound of copper oxide has been intensively studied as a semiconductor material. The most common and stable phases of this semiconductor are CuO (tenorite), which has a monoclinic crystal lattice, and Cu_2O (cuprite), with a cubic structure. Both oxides are being studied as photovoltaic applications because of their reasonable optical properties. CuO is a p-type semiconductor, which according to various data, has a band gap of 1.2 to 2.1 eV, a high absorption coefficient (10^5 cm^{-1}, 300 K), good thermal conductivity (76.5 W mK^{-1}), and electrical resistance, which can range from 10 to 10^5 Ohm·cm depending on the method of production [5–11].

Due to their physical properties, copper oxide (CuO) films have already been used in various fields of science and technology, such as the creation of lithium batteries [12], bio- and gas sensors [13], solar cells [14], capacitors [15], infrared photodetectors [16], catalysis [17], superconductivity [13], for the manufacture of various electrical and optical devices [18,19], etc. However, the most promising applications of CuO, as novel material, are gas sensors and photovoltaic solar cells [20,21].

CuO can be obtained by both physical and chemical methods such as magnetron sputtering [14], molecular beam epitaxy [22], thermal evaporation [23], chemical precipitation [24], polyol process [25], spray pyrolysis [5], sol-gel method [26], solvothermal [27], hydrothermal methods [28], etc. Chemical methods for the synthesis of semiconductor oxides are cheaper, faster, and, as a result, more productive than physical methods. This allows them to scale quite easily for their industrial use.

The spray pyrolysis technique has the next attractive characteristics: cheapness, simplicity, high application rate, and ability to obtain films on large area substrates from various precursors, and therefore it is an effective method of fabricating oxide films with high quality, which allows to precipitate them of varying thickness and size. An essential advantage of this technique is that it does not require a vacuum. In addition, the obtained films are usually homogeneous and are time and temperature stable. The physical properties of the spray-formed CuO thin films can be precisely controlled by adjusting the deposition parameters such as gas flow rate, spray rate, substrate temperature, deposition time, etc. In addition, 3D printers can be equipped with a spray head, which allows, if necessary, the application of semiconductor films on complex three-dimensional surfaces.

It is well-known that functional properties of electronic devices depend on the fundamental characteristics of the applied films that can be changed by deposition regimes [16]. In this regard, we have studied structural and optical properties of CuO films deposited by spraying precursor solution based on copper acetate monohydrate onto glass substrates. The influence of substrate temperature on structural and optical properties of CuO layer films deposited by pulsed spray pyrolysis has been studied in this paper.

2. Materials and Methods

2.1. Chemicals

Chemicals used for obtaining CuO films, copper acetate monohydrate ($Cu(CH_3CO_2)_2 \cdot H_2O$, 99%) and ethanol ($C_2H_5OH$, 95%), were purchased from the company «Sigma Aldrich» (Bratislava, Slovakia).

2.2. Synthesis of CuO Thin Films

CuO thin films were obtained by pulsed spray pyrolysis method. For their fabrication, a solution of copper acetate monohydrate ($Cu(CH_3CO_2)_2 \cdot H_2O$) with a concentration of 0.05 M in distilled water was used as a precursor. Then a few drops of 10% aqueous solution of hydrochloric acid (HCl) were added to the initial solution to increase the degree of solubility of the precursor, which allowed us to maintain the acidity of the pH solution within (6–7) and avoid the formation of copper molecular complexes.

The preparation time of the solution was 10 min under stirring. The resulting solution was sprayed using a jet nozzle onto heated amorphous glass substrates with dimensions of $10 \times 5 \times 1$ mm^3, which were pre-cleaned in an ultrasonic bath for 10 min and washed in ethyl alcohol and then in distilled water. The nozzle diameter was 0.2 mm. The work distance (from the nozzle to the substrate surface) was 17 cm. The spraying rate and the volume of sprayed solution were 2 cm^3/min and 5 cm^3 per sample, respectively. The samples were obtained in the substrate temperature range from T_s = 600 K to 725 K with a step of 25 K.

The spray droplets of precursor evaporate the during transport to the heated substrate. Then the solid precipitate melts and evaporates without decomposition, and the vapor diffuses to the substrate. This leads to the formation of layer of substance on the surface. The compound containing the copper is slowly degraded to form CuO thin film.

At low temperature the droplet splashes onto the substrate and decomposes. At high substrate temperatures the powdery films were produced because of the vaporization and decomposition of the precursor prior to the substrate surface. The optimum temperature the solvent evaporates near substrate surface and adsorbed onto the surface, followed by decomposition to yield a dense film with good adhesion.

2.3. Measurements

The structural characteristics of the deposited films were analyzed by the X-ray diffraction (XRD) method (X-ray diffractometer Bruker D8 Advance, Fremont, CA, USA). The method for calculating structural and substructural properties is described in detail in [29,30]. Additionally, UnitCell (ver. Mar 2021) software was used to determine the lattice parameters, which allows calculations on the position of all diffraction lines from the material [31].

The morphological aspects and the structural quality of samples were probed by scanning electron microscopy (SEM, Jeol, Tokyo, Japan) and atomic force microscopy (AFM, Park XE-100, Park Systems).

Raman measurements were performed using a confocal microscope (Horiba-MTB Xplora, HORIBA France SAS, Kyoto, Japan) at room temperature. The optical properties of CuO films were investigated at room temperature using an Ocean Optics USB4000-UV-VIS fiber optic spectrometer in the wavelength range λ = (300–900) nm. The band gap energy of the obtained films was determined using the method described in detail in [32]. A probe profilometer Dektak XT (Bruker Corporation, Fremont, CA, USA) was used to determine the thickness of the samples.

3. Results and Discussion

3.1. XRD Analysis

To determine the structural features of the CuO thin films the method of XRD analysis was used. The comparing of the diffraction angles and relative intensities of lines from the fabricated thin films and the JCPDS standard were performed to phase analysis. The XRD patterns from CuO thin films are shown in Figure 1, including the reference spectrum from the pure CuO monoclinic phase (JCPDS card No. 00-048-1548) and Cu_2O cubic phase (JCPDS No. 01-078-2076).

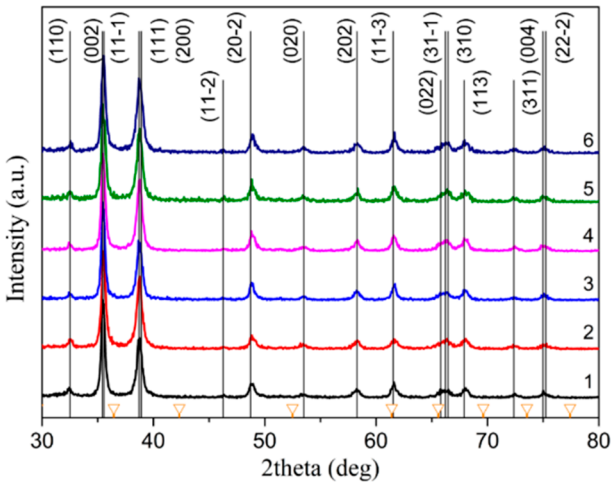

Figure 1. XRD patterns from synthesized CuO films at different substrate temperatures T_s, K: (1) 600, (2) 625, (3) 650, (4) 675, (5) 700, and (6) 725. (Black vertical lines correspond to CuO; orange lines with the triangles show the location of the cubic Cu_2O peaks (JCPDS No. 01-078-2076)).

Figure 1 shows that all XRD patterns contain diffraction peaks located at angles of 32.5° (110), 35.5° (11-1), 38.7° (111), 48.7° (20-2), 53.4° (020), 58.2° (202), 61.5° (11-3), 66.2° (31-1), 68.0° (113), 72.2° (311), and 75.0° (004) that correspond to the specified reflections

from the crystallographic planes [33]. These results are fully consistent with the data of the standard JCPDS card and confirm the monoclinic structure of the fabricated CuO thin film (spatial group C_2/c). No additional peaks of secondary phases and uncontrolled impurities were detected on the XRD patterns. This indicates a reasonably high purity of the obtained thin films, which are single-phase and contain only the CuO phase.

The results of determining the lattice constants of CuO using UnitCell software and obtained by calculations (expressions for calculation are shown in supporting material) are shown in Figure 2a. The solid line shows calculations at a constant value of the angle $\beta = 99°506'$, taken from the reference data (JCPDS card No. 048-1548).

As shown in Figure 2a, the lattice constants a, b, and c of the CuO thin films obtained by calculations are quite close to the reference values. At the same time, the values of the constants obtained using the UnitCell program have much more significant differences with the reference ones and for all the investigated temperatures of the films exceed the calculated values. However, the use of this program allowed us to determine the angle β values of the unit cell of the material, which equals 103.7°. Because of the above, only the calculated results are discussed below.

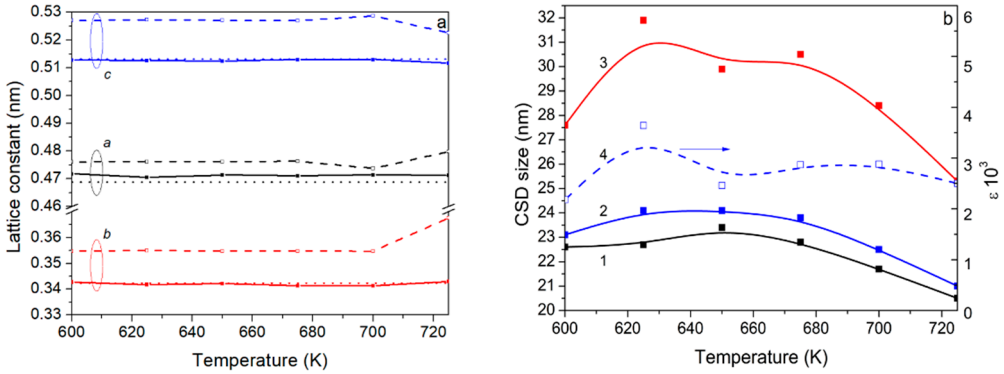

Figure 2. (**a**) Dependence of the lattice constant of the CuO films on the substrate temperature: solid lines correspond to calculation results, dashed-UnitCell software, dotted-reference data; (**b**) effect of the substrate temperature on (4) microstrain level and CSD obtained using (1) Gauss and (3) Cauchi approximation and (2) from threefold convolution.

It is established that when the substrate temperature increases above 625 K, the lattice constant a of the investigated films slightly increases. At the same time, the constant b initially slightly decreases, but the film deposited at T_s = 725 K increases significantly. The constant c, on the contrary, slightly increases with increasing substrate temperature, but for the sample obtained at T_s = 725 K decreases considerably in magnitude. In this the case, the a values were larger, and c values were smaller than those given in the reference JCPDS card.

Based on the results of measuring the lattice constants of the material, we calculated the volume of the unit cell of the obtained samples. The unit cell volume was in the range from 81.22 to 81.78 nm^3.

Calculations of the substructural parameters of CuO thin films were performed in the direction [11-1] of the crystal lattice of the monoclinic phase (by reflection from the plane (11-1) and (22-2)). The coherent scattering domain (CSD) size calculations results by three different methods are summarized in Figure 2b. As can be seen from the Figure 2b, the values of the parameters of the film substructure obtained using different approximations correlate well with each other. This indicates the reliability of the results. However, the most accurate of these are the values obtained by the method of threefold convolution. That is why they will be discussed. The CSD size of the studied films increases from 23.1 nm (T_s = 600 K) to 24.1 nm at 650 K with increasing substrate temperature, and then begins to decrease to 21 nm (T_s = 725 K). Figure 2b (line 4) shows the effect of the substrate temperature on microstrain level in CuO thin films. Presented dependence

of microstrain level was obtained using threefold convolution. Microstrain values with increasing deposition temperature first increased and then decreased. We observed a similar phenomenon in the films of chalcogenides applied by vacuum methods [34].

3.2. Surface Morphology

SEM images of the surface of the synthesized CuO thin films are presented in Figure 3. It can be seen that the nanostructured thin CuO films are quite homogeneous, have a clear polycrystalline structure and a fairly high surface roughness, and also contain small pores. No macroscopic defects, whether exfoliation, voids, or holes, were detected. Figure 3 shows that the grains of the obtained thin films are not homogeneous in size and shape. They acquire spherical, cubic, lamellar, and other shapes. At the same time, those samples deposited at higher substrate temperatures had crystallites predominantly cubic-like cut. Increasing the temperature of the substrate leads to an increase in the size of the crystallites in the thin films, and the average grain diameter is about 90 nm.

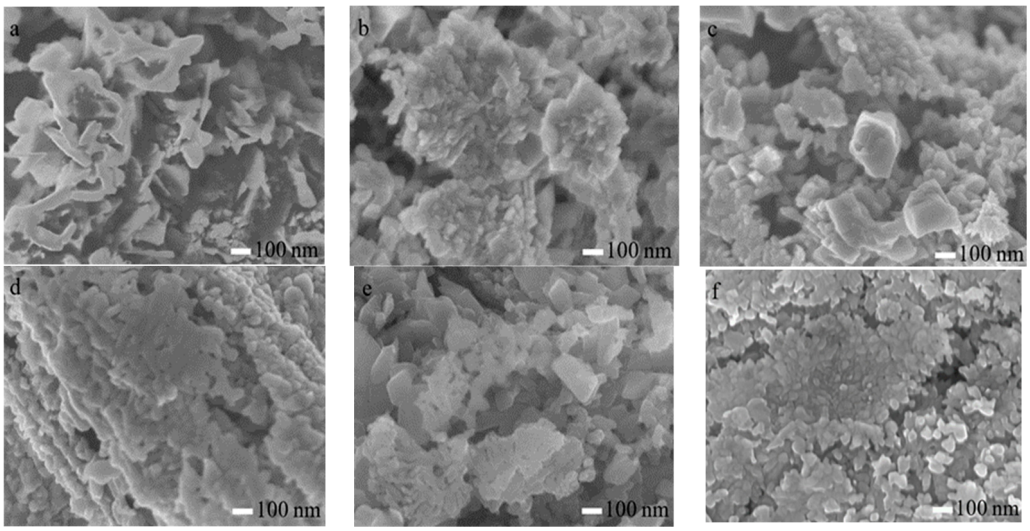

Figure 3. SEM images of the surface of the CuO thin films deposited at different substrate temperatures (50 k magnification), T_s, K: (**a**) 600, (**b**) 625, (**c**) 650, (**d**) 675, (**e**) 700, (**f**) 725.

AFM images of the surface of CuO thin films and their 3D topology are shown in Figure 4. The resulting films have a high homogeneous surface with tightly packed grains. The figure shows that the increasing T_s during obtaining process leads to a grain size increase. The values of R_q the root mean square deviation of their profile from the mean line and R_a average arithmetic roughness were calculated to quantify the surface roughness of the films.

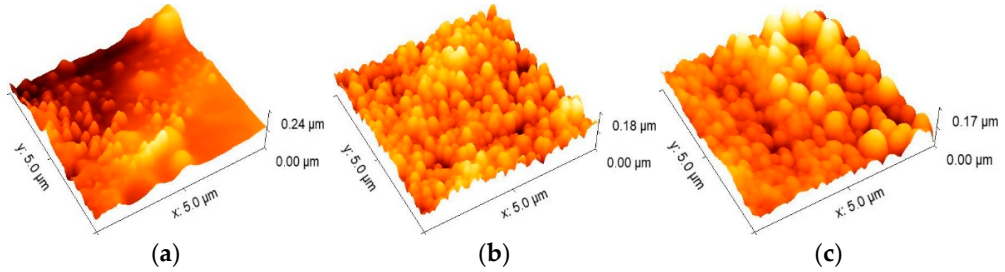

Figure 4. AFM image and 3D topology of the deposited CuO thin films, T_s, K: (**a**) 625, (**b**) 675, (**c**) 725.

Changing the temperature of the substrate affects the roughness of thin films. It was established that increasing of substrate temperature from T_s = 600 K to T_S = 650 K leads to an increase in surface roughness of the thin films (R_a from 15.51 nm to 46.08 nm, R_q from

18.69 nm to 58.12 nm, respectively). Further increase in T_s leads to decrease in the values of R_a and R_q to 19.30 nm and 25.36 nm, respectively.

3.3. Raman Measurements

CuO is a compound that crystallizes into a monoclinic crystal structure. It is described by the space group C_{2h} (C 2/c), where Cu^{2+} ions have four bonds with oxygen [32]. The compound has a four-atom crystallographic cell but contains only two atoms in the primitive cell. Thus, the existence of 12 vibrational modes is possible in the connection. Furthermore, two copper atoms in a primitive cell are in states with symmetry, described as $C_1(2)$, and an oxygen atom in $C_2(2)$ [35].

The optical phonon modes of the compound relative to the center of the Brillouin zone are given by the expression $\Gamma_{RA} = 4A_u + 5B_u + A_g + 2B_g$, where Γ is the degree of freedom of vibrations, A_u and B_u correspond to infrared modes, and A_g and B_g correspond to Raman modes. Thus, we have six infrared active modes ($3A_u + 3B_u$), three of which belong to acoustic ($A_u + 2B_u$ modes), and three to Raman scattering ($A_g + 2B_g$ modes) [36–38].

Figure 5a shows the Raman spectra of CuO thin films deposited at different substrate temperatures in the frequency range from 180 cm^{-1} to 800 cm^{-1}. For the synthesized films, the Raman peaks at frequencies 268, 320, and 604 cm^{-1} correspond to the modes A_{1g}, B_{1g}, and B_{2g} of the crystal structure of monoclinic CuO, respectively. The obtained frequencies correlate with those given in the reference [39,40]. Peaks at frequencies of about 430 cm^{-1} and 505 cm^{-1} correspond to peaks in the spectra from the substrate.

It is known that the intensity of Raman peaks depends on the grain size. The most intense mode A_{1g} (268 cm^{-1}), which characterizes the monoclinic structure of CuO, is present in the spectra of all deposited films. The shift of the position of the peaks in different samples (Figure 5b) indicates the presence in the films of microstresses, which may be due to the presence of one-dimensional defects associated with the presence of oxygen vacancies and two-dimensional defects (dislocations) that deform the lattice [41].

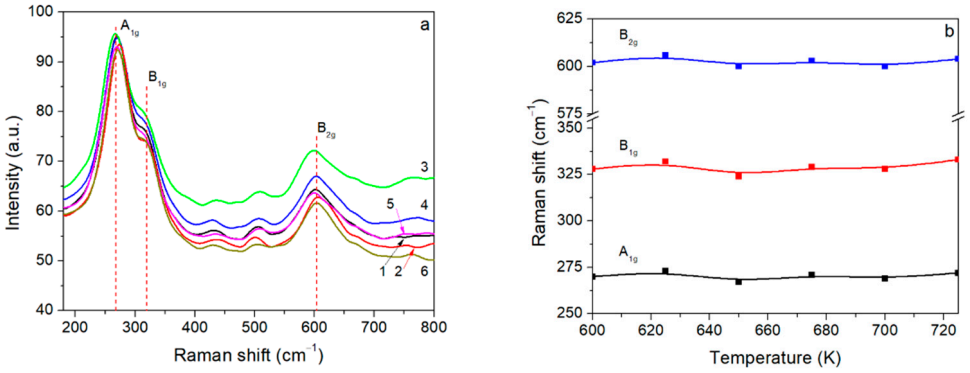

Figure 5. (**a**) Raman spectra of CuO films obtained at different temperatures and (**b**) peaks shift of the films, T_s, K: (1) 600, (2) 625, (3) 650, (4) 675, (5) 700, (6) 725.

3.4. Optical Properties

Figure 6 shows the transmittance and absorbance spectra of films taken in UV and the visible wavelength range λ = (300–900) nm. It is established that CuO thin films have a high absorbance in the visible spectrum (85–90%), which decreases with increasing wavelength. The highest values of the absorbance are observed for films deposited at a higher substrate temperature.

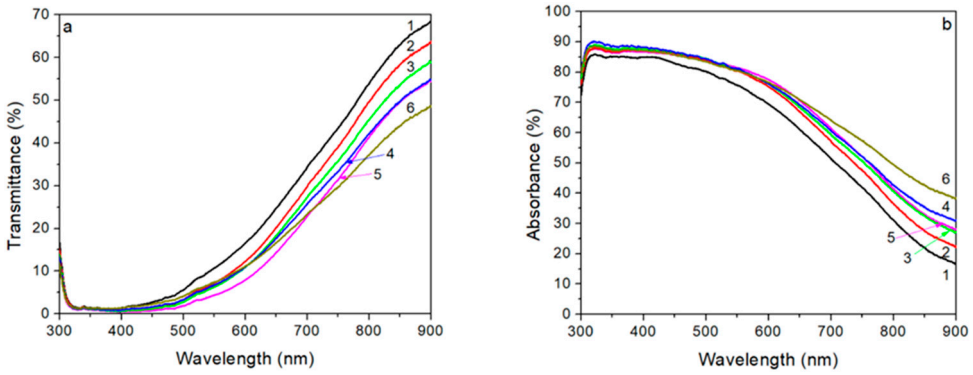

Figure 6. (**a**) Transmittance and (**b**) absorbance spectra of CuO thin films obtained at different temperatures, T_s, K: (1) 600, (2) 625, (3) 650, (4) 675, (5) 700, (6) 725.

Figure 7a shows the dependences $(\alpha hv)^2$-(hv) used to determine the optical band gap of the synthesized CuO thin films. The calculated energy of the optical band gap CuO in the case of direct transitions is in the range (1.45–1.60) eV (Figure 7b). These values are significantly higher than those given in the reference data for bulk CuO [18,24,42].

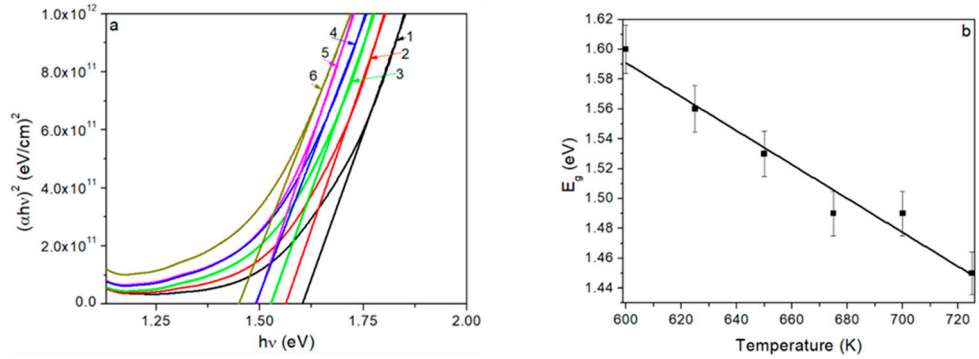

Figure 7. (**a**) The dependences $(\alpha hv)^2$-(hv) constructed for CuO thin films obtained at different temperatures, T_s, K: (1) 600, (2) 625, (3) 650, (4) 675, (5) 700, (6) 725; (**b**) band gap energy variation with the substrate temperature of CuO thin films.

It is known that the change in E_g of the film material may be due to the presence of defects, small grain size, semiconductor degeneracy, etc. [43,44]. Thus, the change of the material's band gap indicates a difference in the quality of the thin films applied at different deposition temperatures. The obtained band gap values are similar to the values determined for CuO films presented in the works of other researchers [45].

The band gap energy increases with decreasing size of the nanostructured material, and discrete energy levels appear in the band. When photons fall on semiconductor material, they will be absorbed only when the minimum photon energy is sufficient to excite the electron. Of course, the band gap energy of nanostructured CuO thin films is greater than the energy of the bulk material [42,46].

In addition, thin film resistance was analyzed by Van Der Pauw using four small In contacts placed on the corners of the square on the top of the thin film. It has been found that resistance is reduced linearly from 12 Ohm·cm to 5.9 Ohm·cm for 600 to 725 K, respectively. For resistivity calculation an average thickness ~1000 nm was used.

4. Conclusions

Thin films of CuO were deposited by pulsating spray pyrolysis method. The influence of substrate temperature on morphological, structural, and optical properties was determined.

Based on XRD analysis, it was determined that the CuO thin films are single-phase. AFM and SEM measurements showed that the obtained films have a reasonably high surface roughness. An increase in the substrate temperature leads to an increase in grain size in the obtained thin films.

Raman spectroscopy revealed three modes A_{1g}, B_{1g}, and B_{2g} of the crystal structure of monoclinic CuO. Peak shifts in different samples indicate the presence of microstresses and defects that violate the CuO lattice.

It is established that the obtained thin films of CuO have high values of the absorption coefficient, which confirms the possibility of using them as an absorbing layer in solar cells. Furthermore, the optical band gap of CuO thin films, ranging from 1.45 eV to 1.60 eV, was determined. The discrepancy between the values of the band gap relative to the values for the bulk material may be due to the presence of defects or changes in grain size in thin films, which can be considered the main factors of changing the band gap of deposited CuO thin films.

Author Contributions: O.D. (Oleksii Diachenko): conceptualization, writing—original draft, and visualization. J.K.J.: resources, writing—review and editing, and project administration. O.D. (Oleksandr Dobrozhan): resources and investigation. P.N.: formal analysis and investigation. J.K.: methodology and supervision. J.S.: investigation. A.O.: methodology and supervision. All authors have read and agreed to the published version of the manuscript.

Funding: This research was funded by the National Research Foundation of Ukraine (grant number: 0120U104809). This research was also funded by Slovak Agency for Science and Development (project no. APVV-20-0437) and Grant through the Ministry of Education, Science, Research, and Sport of Slovakia (project no. VEGA 1/0733/20). O.D. thanks the National Scholarship Program of the Slovak Republic (SAIA) for his research stay grant at the Slovak University of Technology in Bratislava.

Institutional Review Board Statement: Not applicable.

Informed Consent Statement: Not applicable.

Data Availability Statement: shorturl.at/mosCQ.

Conflicts of Interest: The authors declare no conflict of interest. The funders had no role in the design of the study; in the collection, analyses, or interpretation of data; in the writing of the manuscript, or in the decision to publish the results.

References

1. Kim, M.S.; Yim, K.G.; Leem, J.Y.; Kim, S.; Nam, G.; Lee, D.Y.; Kim, J.S. Thickness dependence of properties of ZnO thin films on porous silicon grown by plasma-assisted molecular beam epitaxy. *J. Korean Phys. Soc.* **2011**, *59*, 2354–2361. [CrossRef]
2. Sawicka-Chudy, P.; Sibiński, M.; Rybak-Wilusz, E.; Cholewa, M.; Wisz, G.; Yavorskyi, R. Review of the development of copper oxides with titanium dioxide thin-film solar cells. *AIP Adv.* **2020**, *10*, 010701. [CrossRef]
3. Pavan, M.; Rühle, S.; Ginsburg, A.; Keller, D.A.; Barad, H.N.; Sberna, P.M.; Fortunato, E. TiO_2/Cu_2O all-oxide heterojunction solar cells produced by spray pyrolysis. *Sol. Energy Mater. Sol. Cells* **2015**, *132*, 549–556. [CrossRef]
4. Morasch, J.; Li, S.; Brötz, J.; Jaegermann, W.; Klein, A. Reactively magnetron sputtered Bi2O3 thin films: Analysis of structure, optoelectronic, interface, and photovoltaic properties. *Phys. Status Solidi A* **2014**, *211*, 93–100. [CrossRef]
5. Moumen, A.; Hartiti, B.; Comini, E.; Arachchige, H.M.M.; Fadili, S.; Thevenin, P. Preparation and characterization of nanostructured CuO thin films using spray pyrolysis technique. *Superlattices Microstruct.* **2019**, *127*, 2–10. [CrossRef]
6. Naveena, D.; Logu, T.; Dhanabal, R.; Sethuraman, K.; Bose, A.C. Comparative study of effective photoabsorber CuO thin films prepared via different precursors using chemical spray pyrolysis for solar cell application. *J. Mater. Sci. Mater. Electron.* **2019**, *30*, 561–572. [CrossRef]
7. Ooi, P.K.; Ng, S.S.; Abdullah, M.J.; Hassan, H.A.; Hassan, Z. Effects of oxygen percentage on the growth of copper oxide thin films by reactive radio frequency sputtering. *Mater. Chem. Phys.* **2013**, *140*, 243–248. [CrossRef]
8. Shabu, R.; Raj, A.M.E.; Sanjeeviraja, C.; Ravidhas, C. Assessment of CuO thin films for its suitablity as window absorbing layer in solar cell fabrications. *Mater. Res. Bull.* **2015**, *68*, 1–8. [CrossRef]
9. Valladares, L.D.L.S.; Salinas, D.H.; Dominguez, A.B.; Najarro, D.A.; Khondaker, S.I.; Mitrelias, T.; Majima, Y. Crystallization and electrical resistivity of Cu_2O and CuO obtained by thermal oxidation of Cu thin films on SiO_2/Si substrates. *Thin Solid Films* **2012**, *520*, 6368–6374. [CrossRef]
10. Li, Y.; Tung, S.; Schneider, E.; Xi, S. A review on development of nanofluid preparation and characterization. *Powder Technol.* **2009**, *196*, 89–101. [CrossRef]

11. Zoolfakar, A.S.; Rani, R.A.; Morfa, A.J.; O'Mullane, A.P.; Kalantar-Zadeh, K. Nanostructured copper oxide semiconductors: A perspective on materials, synthesis methods and applications. *J. Mater. Chem. C* **2014**, *2*, 5247–5270. [CrossRef]
12. Deng, Z.; Ma, Z.; Li, Y.; Li, Y.; Chen, L.; Yang, X.; Su, B.L. Boosting lithium-ion storage capability in CuO nanosheets via synergistic engineering of defects and pores. *Front. Chem.* **2018**, *6*, 428. [CrossRef] [PubMed]
13. Ehsani, M.; Chaichi, M.J.; Hosseini, S.N. Comparison of CuO nanoparticle and CuO/MWCNT nanocomposite for amplification of chemiluminescence immunoassay for detection of the hepatitis B surface antigen in biological samples. *Sens. Actuators B Chem.* **2017**, *247*, 319–328. [CrossRef]
14. Dolai, S.; Dey, R.; Das, S.; Hussain, S.; Bhar, R.; Pal, A.K. Cupric oxide (CuO) thin films prepared by reactive dc magnetron sputtering technique for photovoltaic application. *J. Alloys Compd.* **2017**, *724*, 456–464. [CrossRef]
15. Hilman, J.; Yost, A.J.; Tang, J.; Leonard, B.; Chien, T. Low temperature growth of CuO nanowires through direct oxidation. *Nano-Struct. Nano-Objects* **2017**, *11*, 124–128. [CrossRef]
16. Wang, S.B.; Hsiao, C.H.; Chang, S.J.; Lam, K.T.; Wen, K.H.; Hung, S.C.; Huang, B.R. A CuO nanowire infrared photodetector. *Sens. Actuators A* **2011**, *171*, 207–211. [CrossRef]
17. Zhou, K.; Li, Y. Catalysis based on nanocrystals with well-defined facets. *Angew. Chem. Int. Ed.* **2012**, *51*, 602–613. [CrossRef] [PubMed]
18. Diachenko, O.V.; Dobrozhan, O.A.; Opanasyuk, A.S.; Ivashchenko, M.M.; Protasova, T.O.; Kurbatov, D.I.; Čerškus, A. The influence of optical and recombination losses on the efficiency of thin-film solar cells with a copper oxide absorber layer. *Superlattices Microstruct.* **2018**, *122*, 476–485. [CrossRef]
19. Chavali, M.S.; Nikolova, M.P. Metal oxide nanoparticles and their applications in nanotechnology. *SN Appl. Sci.* **2019**, *1*, 1–30. [CrossRef]
20. Dhas, C.R.; Alexander, D.; Christy, A.J.; Jeyadheepan, K.; Raj, A.M.E.; Raja, C.S. Preparation and characterization of CuO thin films prepared by spray pyrolysis technique for ethanol gas sensing application. *Asian J. Appl. Sci.* **2014**, *7*, 671–684. [CrossRef]
21. Gopalakrishna, D.; Vijayalakshmi, K.; Ravidhas, C. Effect of pyrolytic temperature on the properties of nano-structured CuO optimized for ethanol sensing applications. *J. Mater. Sci. Mater. Electron.* **2013**, *24*, 1004–1011. [CrossRef]
22. Yang, K.G.; Hu, P.; Wu, S.X.; Ren, L.Z.; Yang, M.; Zhou, W.Q.; Li, S.W. Room-temperature ferromagnetic CuO thin film grown by plasma-assisted molecular beam epitaxy. *Mater. Lett.* **2016**, *166*, 23–25. [CrossRef]
23. Sahu, K.; Choudhary, S.; Khan, S.A.; Pandey, A.; Mohapatra, S. Thermal evolution of morphological, structural, optical and photocatalytic properties of CuO thin films. *Nano-Struct. Nano-Objects* **2019**, *17*, 92–102. [CrossRef]
24. Sagadevan, S.; Pal, K.; Chowdhury, Z.Z. Fabrication of CuO nanoparticles for structural, optical and dielectric analysis using chemical precipitation method. *J. Mater. Sci. Mater. Electron.* **2017**, *28*, 12591–12597. [CrossRef]
25. Dobrozhan, O.; Vorobiov, S.; Kurbatov, D.; Baláž, M.; Kolesnyk, M.; Opanasyuk, A. Structural properties and chemical composition of ZnO films deposited onto flexible substrates by spraying polyol mediated nanoinks. *Superlattices Microstruct.* **2020**, *140*, 106455. [CrossRef]
26. Lim, Y.F.; Chua, C.S.; Lee, C.J.J.; Chi, D. Sol–gel deposited Cu 2 O and CuO thin films for photocatalytic water splitting. *Phys. Chem. Chem. Phys.* **2014**, *16*, 25928–25934. [CrossRef] [PubMed]
27. Hong, J.; Li, J.; Ni, Y. Urchin-like CuO microspheres: Synthesis, characterization, and properties. *J. Alloys Compd.* **2009**, *481*, 610–615. [CrossRef]
28. Ozga, M.; Kaszewski, J.; Seweryn, A.; Sybilski, P.; Godlewski, M.; Witkowski, B.S. Ultra-fast growth of copper oxide (II) thin films using hydrothermal method. *Mater. Sci. Semicond. Process.* **2020**, *120*, 105279. [CrossRef]
29. Diachenko, O.V.; Opanasiuk, A.S.; Kurbatov, D.I.; Cheong, H.; Kuznetsov, V.M. Effect of substrate temperature on structural and substructural properties of MgO thin films. *Funct. Mater.* **2015**, *22*, 487–493. [CrossRef]
30. Umanskij, J.S.; Skakov, J.A.; Ivanov, A.N.; Rastorgujev, L.N. *Crystallogaphy, X-ray Graph and Electronmicroscopy*; Metallurgy: Moskow, Russia, 1982.
31. Holland, T.J.B.; Redfern, S.A.T. Unitcell: A nonlinear least-squares program for cell-parameter refinement and implementing regression and deletion diagnostics. *J. Appl. Crystallogr.* **1997**, *30*, 84. [CrossRef]
32. Dobrozhan, O.; Kurbatov, D.; Opanasyuk, A.; Cheong, H.; Cabot, A. Influence of substrate temperature on the structural and optical properties of crystalline ZnO films obtained by pulsed spray pyrolysis. *Surf. Interface Anal.* **2015**, *47*, 601–606. [CrossRef]
33. Akgul, F.A.; Akgul, G.; Yildirim, N.; Unalan, H.E.; Turan, R. Influence of thermal annealing on microstructural, morphological, optical properties and surface electronic structure of copper oxide thin films. *Mater. Chem. Phys.* **2014**, *147*, 987–995. [CrossRef]
34. Opanasyuk, A.S.; Kurbatov, D.I.; Kosyak, V.V. Characteristics of structure formation in zinc and cadmium chalcogenide films deposited on nonorienting substrates. *Crystallogr. Rep.* **2012**, *57*, 927–933. [CrossRef]
35. Åsbrink, S.; Norrby, L.J. A refinement of the crystal structure of copper (II) oxide with a discussion of some exceptional esd's. *Acta crystallogr. B Struct. Crystallogr. Cryst. Chem.* **1970**, *26*, 8–15. [CrossRef]
36. Mageshwari, K.; Sathyamoorthy, R. Flower-shaped CuO nanostructures: Synthesis, characterization and antimicrobial activity. *J. Mater. Sci. Technol.* **2013**, *29*, 909–914. [CrossRef]
37. Maji, S.K.; Mukherjee, N.; Mondal, A.; Adhikary, B.; Karmakar, B. Chemical synthesis of mesoporous CuO from a single precursor: Structural, optical and electrical properties. *J. Solid State Chem.* **2010**, *183*, 1900–1904. [CrossRef]
38. Wang, X.; Xi, G.; Xiong, S.; Liu, Y.; Xi, B.; Yu, W.; Qian, Y. Solution-phase synthesis of single-crystal CuO nanoribbons and nanorings. *Cryst. Growth Des.* **2007**, *7*, 930–934. [CrossRef]

39. Murthy, P.S.; Venugopalan, V.P.; Arunya, D.D.; Dhara, S.; Pandiyan, R.; Tyagi, A.K. Antibiofilm activity of nano sized CuO. In Proceedings of the IEEE International Conference on Nanoscience, Engineering and Technology, Chennai, India, 28–30 November 2011; pp. 580–583.
40. Hinna, M.; Hartiti, B.; Batan, A.; Reniers, F.; Buess-Herman, C.; Segato, T.; Thévenin, P. Elaboration and Characterization of CuO Thin Films by Spray Pyrolysis Method for Gas Sensors Applications. *Multidiscip. Digit. Publ. Inst. Proc.* **2019**, *14*, 55. [CrossRef]
41. Arguello, C.A.; Rousseau, D.L.; Porto, S.D.S. First-order Raman effect in wurtzite-type crystals. *Phys. Rev.* **1969**, *181*, 1351. [CrossRef]
42. Murali, D.S.; Kumar, S.; Choudhary, R.J.; Wadikar, A.D.; Jain, M.K.; Subrahmanyam, A. Synthesis of Cu_2O from CuO thin films: Optical and electrical properties. *AIP Adv.* **2015**, *5*, 047143. [CrossRef]
43. Sengupta, J.; Sahoo, R.K.; Bardhan, K.K.; Mukherjee, C.D. Influence of annealing temperature on the structural, topographical and optical properties of sol–gel derived ZnO thin films. *Mater. Lett.* **2011**, *65*, 2572–2574. [CrossRef]
44. Hong, R.; Huang, J.; He, H.; Fan, Z.; Shao, J. Influence of different post-treatments on the structure and optical properties of zinc oxide thin films. *Appl. Surf. Sci.* **2005**, *242*, 346–352. [CrossRef]
45. Koffyberg, F.P.; Benko, F.A. A photoelectrochemical determination of the position of the conduction and valence band edges of p-type CuO. *J. Appl. Phys.* **1982**, *53*, 1173–1177. [CrossRef]
46. Dhineshbabu, N.R.; Rajendran, V.; Nithyavathy, N.; Vetumperumal, R. Study of structural and optical properties of cupric oxide nanoparticles. *Appl. Nanosci.* **2016**, *6*, 933–939. [CrossRef]